Available online at www.sciencedirect.com

ScienceDirect

Procedia Engineering 213 (2018) 674–681

Procedia Engineering

www.elsevier.com/locate/procedia

7th International Conference on Fatigue Design, Fatigue Design 2017, 29-30 November 2017, Senlis, France

Corrosion Fatigue of Low Carbon Steel under Compressive Residual Stress Field

Volodymyr Okorokov[a,]*, Marta Morgantini[a], Yevgen Gorash[a], Tugrul Comlekci[b], Donald Mackenzie[a] and Ralph van Rijswick[c]

[a]*University of Strathclyde, 99 George St, Glasgow, G1 1RD, UK*
[b] *University of the West of Scotland, High Street, Paisley, PA1 2BE, UK*
[c]*Weir Minerals, Venlo, 5928 PH, NL*

Abstract

This paper presents experimental investigation and numerical modeling of the effect of compressive residual stress on the corrosion fatigue life of a low carbon steel. A fatigue life test methodology based on double notched tensile test specimens is proposed. A new plasticity model is proposed for accurate simulation of compressive residual stress and calibrated to experimental stress-strain curves obtained for low carbon steel. The proposed model is implemented as a user-material in the ANSYS Workbench Finite Element Analysis program and utilized in plastic analysis and fatigue assessment. Corrosion fatigue test results are discussed and compared to numerical predictions.

Peer-review under responsibility of the scientific committee of the 7th International Conference on Fatigue Design.

Keywords: Corrosion fatigue; Autofrettage; Crack arrest; Compressive residual stress; Cyclic plasticity

1. Introduction

Corrosion fatigue failure is a fundamental design consideration in industries where plant and structures are subject to cyclic loading in a corrosive environment. In many applications, this is addressed through manufacture in corrosion resistant base materials, such as stainless steels, or incorporating barrier linings or coatings to protect the

* Corresponding author. Tel.: +44-787-427-54-42;
E-mail address: volodymyr.okorokov@strath.ac.uk

1877-7058
Peer-review under responsibility of the scientific committee of the 7th International Conference on Fatigue Design.
10.1016/j.proeng.2018.02.063

base material from corrosive attack. However, these approaches are not always appropriate for cost or technical reasons. In such cases, an alternative approach may be to enhance resistance to corrosion fatigue failure by inducing compressive residual stress in highly loaded regions of the structure.

Residual stress methods such as shot peening, low plasticity burnishing, laser peening, deep rolling and autofrettage are used in a variety of industries to improve fatigue life. The motivation for the work presented here is to develop greater understanding of the autofrettage process in pump applications but it is also relevant to use of other residual stress methods in other applications.

Autofrettage is used to improve fatigue performance of pressure retaining structures, such as pressure vessel, gun barrels and pump fluid ends. Compressive residual stress is established by initially subjecting the component to an internal pressure great enough to cause plastic deformation in highly loaded regions. This reduces the local mean stress in these regions under operating conditions [1-5], increasing crack initiation time and fatigue life. The compressive stress field may also arrest growth of the crack after initiation [6, 7].

The effect of autofrettage residual stress on corrosion fatigue behavior *per se* has not previously been reported in the literature to a notable extent. Cyclic loading of carbon steel in a corrosive environment is widely known to significantly reduce the number of cycles to failure compared to a non-corrosive environment. Further, the material does not exhibit the fatigue (or endurance) limit behavior observed in tests in dry air. This paper presents an experimental investigation of the effect of residual stress on fatigue life of a carbon steel in a corrosive environment.

Experimental investigation of the fatigue life of autofrettaged components in pressure test rigs, as in [8], requires access to specialist facilities. This type of testing is relatively expensive and appropriate as a final step in designing a new pressure component. Here, a simpler and less expensive experimental method is proposed, based on tensile tests of double notched square cross-section specimens. A residual stress field is induced in the specimen prior to fatigue testing by initially loading the specimen so as to cause plastic deformation in the notch region, such that a compressive residual stress field is established upon subsequently unloading to zero axial force. The experimental results are simulated and analyzed in terms of a proposed new plasticity material model and the theory of critical distance [9].

2. Modelling Compressive Residual Stress

The autofrettage residual stress field arises from plastic deformation of the component during initial loading beyond first yield and subsequent unloading. Accurate prediction of the residual stress field therefore requires a mathematical material model of the plastic deformation that incorporates the material cyclic plasticity response.

2.1. Cyclic Plasticity Testing

The material considered in the investigation is a general purpose low carbon steel with nominal yield stress 260 MPa and Tensile Strength 500 MPa. Monotonic and cyclic stress strain curves for the material were obtained through tensile testing of rectangular test specimens of total length 140 mm, gauge length 25 mm, grip section width 20 mm, gauge section width 12 mm and thickness 6 mm. The tests were conducted on a 250 kN INSTRON servo-hydraulic testing machine under strain control, with a total strain rate of $5E^{-4}$ s^{-1} for both monotonic and cyclic loading. Strain was measured using a 10 mm gauge length extensometer.

The cyclic plastic behaviour of the material for non-zero mean strain is shown in Figure 1. The results exhibit important cyclic plasticity phenomena such as the Bauschinger effect, cyclic mean stress relaxation and elastic property degradation with accumulation of plastic strain. This behaviour is of specific relevance to autofrettage as it captures a realistic material response similar to that experienced in application of the autofrettage process.

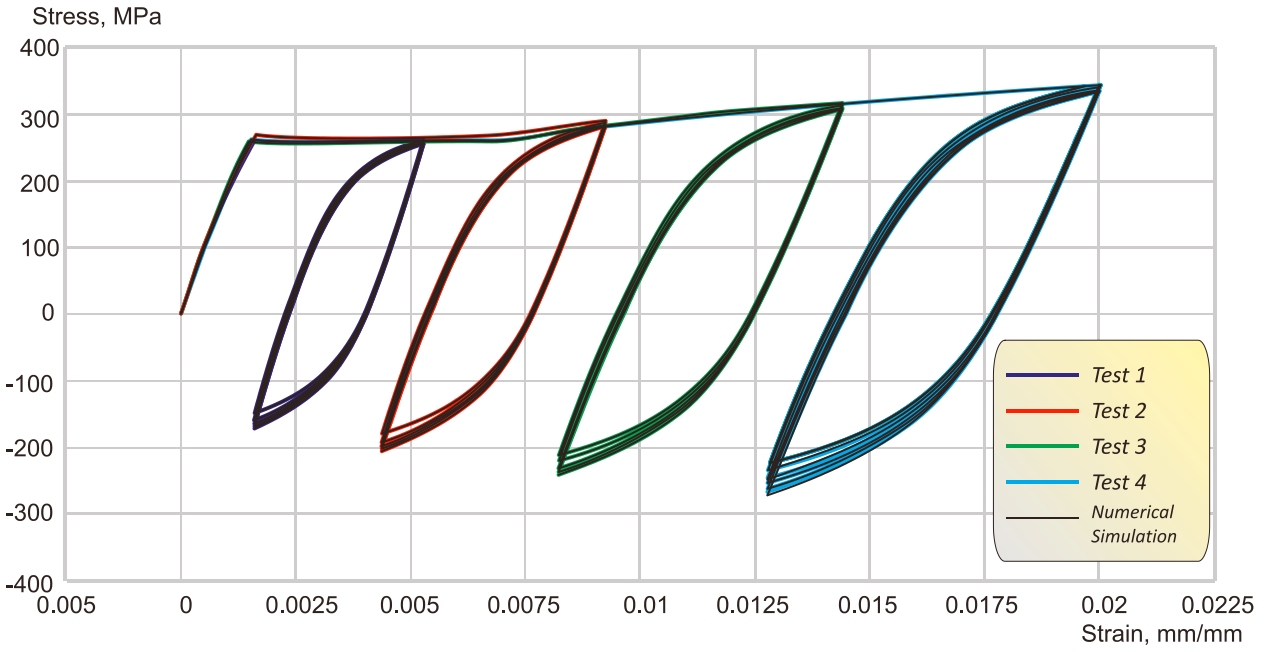

Fig. 1. Cyclic plasticity material response.

2.2. Cyclic Plasticity Constitutive Modelling

Modelling the cyclic plasticity response of Figure 1 requires an appropriate plasticity model. Here a cyclic plasticity constitutive model based on the von Mises yield criterion is proposed for that purpose. The yield surface is implemented as:

$$f = \sqrt{\frac{3}{2}(\mathbf{S}-\mathbf{X}):(\mathbf{S}-\mathbf{X})} - R - \sigma_0 \tag{1}$$

The phenomena of cyclic softening and hardening suggest that stable hysteresis loops are achieved after cycling under a fixed strain range. The experimental observations from Figure 1 show a strong dependence between stabilized stress peaks and strain ranges, or non-Masing behaviour. To describe this type of material behaviour, Chaboche et al. [10] proposed an internal variable introducing a dependence of the isotropic hardening asymptotic value on the plastic strain range. The memory surface is introduced by:

$$F = \sqrt{(\boldsymbol{\varepsilon}^{\mathbf{p}} - \boldsymbol{\zeta})(\boldsymbol{\varepsilon}^{\mathbf{p}} - \boldsymbol{\zeta})} - q \tag{2}$$

where $\boldsymbol{\varepsilon}^{\mathbf{p}}$ is the plastic strain tensor and $\boldsymbol{\zeta}$ and q are the centre and the radius of the memory surface, respectively. Nouailhas et al. [11] and Ohno [12] introduced a fading function into the variable q to provide better agreement with experiments.

Although this form of constitutive model can describe a cyclic stress-strain curve precisely, there are associated disadvantages. The shape of the monotonic curve and the shape of each curve from cyclic loading are fully determined by a single unified set of equations and parameters calibrated for a cyclic stress-strain curve. Consequently, the monotonic curves for the first cycles will be different from experimental results. To overcome this problem and describe all stress-strain curves for cyclic loading, from the monotonic curve to the saturation of stresses, a new set of internal variables is proposed:

$$\dot{\bar{q}} = [p - \bar{p}' - 2\bar{q}']\delta(Z)\dot{p} \qquad \dot{\bar{p}} = [p - \bar{p}']\delta(Z)\dot{p} \tag{3}$$

where $\dot{\bar{q}}$ is the rate of strain amplitude attained in the previous step, $\dot{\bar{p}}$ is the rate of accumulated plastic strain attained during straining to the end of the previous step and the Dirac delta function of the argument δ is defined as:

$$Z = \frac{1}{2}\left[p - p' - \text{sign}(\varepsilon_{eq}^{p} - \bar{\varepsilon}_{eq}^{p})(\varepsilon_{eq}^{p} - \varepsilon_{eq}'^{p})\right] \qquad \varepsilon_{eq}^{p} = \sqrt{\frac{2}{3}\boldsymbol{\varepsilon}^{\mathbf{p}} : \boldsymbol{\varepsilon}^{\mathbf{p}}} \tag{4}$$

$$\bar{q}' = \bar{q}(t-\tau) \qquad p' = p(t-\tau) \qquad \bar{p}' = \bar{p}(t-\tau) \qquad \varepsilon_{eq}'^{p} = \varepsilon_{eq}^{p}(t-\tau) \tag{5}$$

where τ is the infinitesimal time delay. The main feature of the delay differential equations is that the Dirac function returns a required value only at the beginning of a new step. At other times the Dirac function returns a zero value and the variables remain unchanged during the plastic deformation. This allows the new variables to be constants on the current load step and change in value only at the beginning of the next step. Strain range dependence is introduced into the constants through isotropic and kinematic hardening rules.

2.3. Compressive Residual Stress Simulation

The double notch test specimen geometry used in the material tests is shown in Figure 2. Compressive residual stress is induced in the specimen notch region prior to fatigue testing. The specimen is mounted in the test machine and axial loading applied such that plastic deformation first occurs in the notch intersection or corner regions, the locations of maximum stress concentration, and spreads into the specimen by a controlled amount such that the core of the specimen remains elastic. When the axial load is subsequently reduced to zero, a self-equilibrating state of stress is established in the specimen, with tensile residual stress in the elastic core and compressive residual stress in the regions where plastic deformation had occurred.

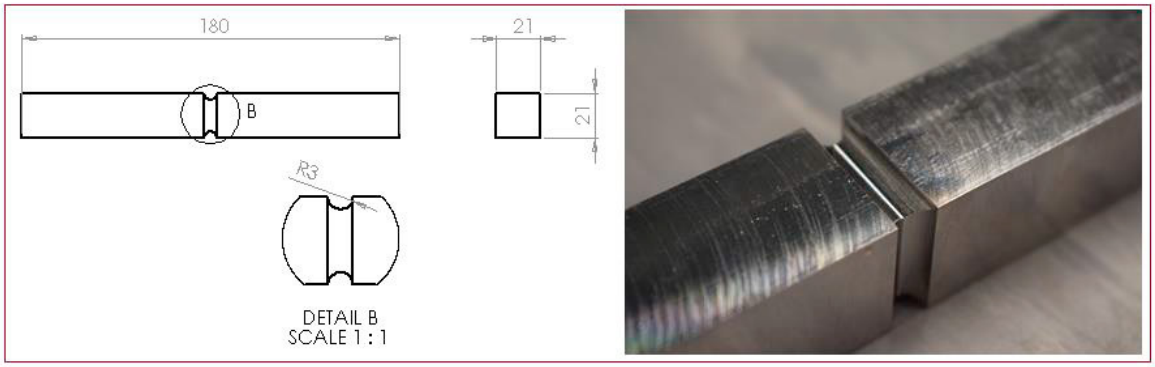

Fig. 2. Double notched sample geometry, dimensions mm.

The initial deformation process and resulting residual stress was investigated by Finite Element Analysis using the ANSYS Workbench program. The new plasticity model proposed in Section 2.2 above was implemented in ANSYS Workbench as a User Programmable Feature (UPF), wherein the user may implement custom equations and solving algorithms.

Contour plots of calculated maximum compressive (principal) residual stress in the specimen for loading to 75 kN and unloading to zero are shown in Figure 3. The results given by the new plasticity model are shown in Figure 3a. Results obtained for the same model using the standard ANSYS elastic-perfectly plastic and Chaboche nonlinear kinematic hardening material models are shown in Figures 3b and 3c respectively. The results of the three analyses show significantly different magnitudes and distributions of calculated compressive residual stresses These differences are attributed to the inability of the standard models to fully describe the material stress-strain relationship during the unloading stage of the load cycle. In practical simulation of autofrettage procedures in the context of fatigue analysis, overestimation of the compressive residual stresses may result in non-conservative evaluation of fatigue life.

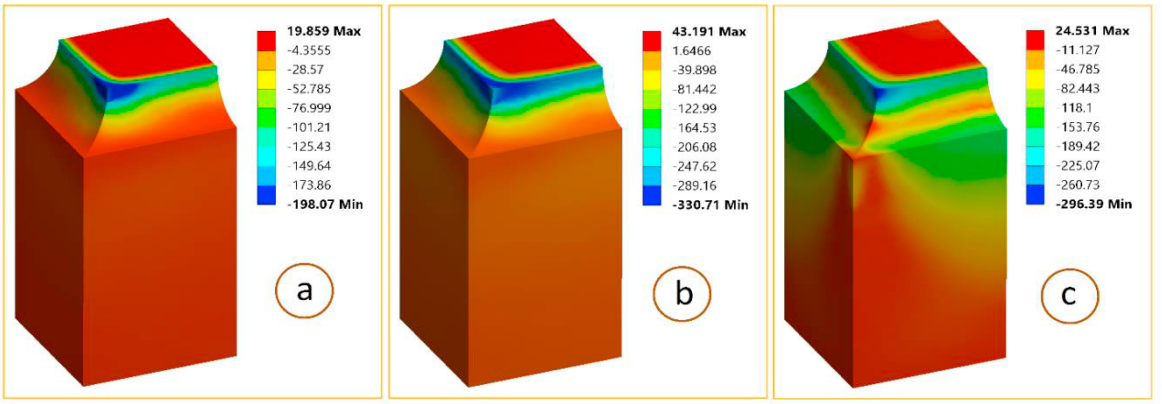

Fig. 3. Compressive residual stress field (minimum principal stress) after unloading by a) proposed plasticity model; b) perfectly plastic material; c) nonlinear Chaboche kinematic hardening.

The Finite Element contour plots of Figure 3 results show that the form of the compressive residual stress field established in the doubled notched specimen prior to fatigue testing is similar to that occurring in autofrettaged pressure parts with structural discontinuities such as cross-bores. The specimen design therefore provides a representative model of the effect of compressive residual stress in autofrettaged components when cyclic loading is applied.

3. Fatigue Testing

Fatigue testing of standard and double notched material specimens was performed to investigate the fatigue life of the low carbon steel considered.

3.1. Fatigue Testing of Standard Specimens

Uniaxial fatigue tests were conducted for round specimens with geometry parameters: total length 274 mm; gauge length 24 mm; grip section diameter 16 mm; gauge section diameter 6 mm. The tests were performed on a 100 kN INSTRON servo-hydraulic testing machine under the force control at frequency 10 Hz and 15 Hz. The load ratio considered were R = 0, R = -1 and R = -8.3. Tests were performed in air and tap water environments at room temperature.

The results of the fatigue tests are presented in Figure 4 in the form of a Haigh diagram. It can be seen that the material fatigue strength varies with the load cycle mean stress. The blue line represents infinite fatigue life of the specimens tested in air. The red line represents a corrosion fatigue life of 3E6 cycles in tap water. It is seen that the corrosion environment greatly decreases the fatigue strength of the plain uniaxial samples.

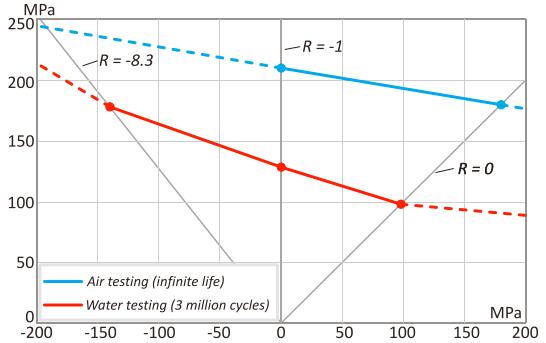

Fig. 4. Haigh diagram for the uniaxial fatigue testing in the water and air environment

3.2. Fatigue Testing of Double Notched Specimens

Fatigue testing of autofrettaged components in in pressure test rigs requires specialist facilities and can be prohibitively expensive. The test methodology proposed and used here considers the behavior of a double notched tensile test specimen, as defined in Figure 2, in which a representative compressive residual stress field is induced through pre-test overloading. A range of values of maximum compressive residual stresses were induced in specimen notch region using a 250 kN INSTRON servo-hydraulic machine by applying overload cycles of axial forces in the range of *55 kN – 130 kN*, 60 s loading and 60 s unloading. The loading ratio of the applied remote force was $R = 0$ for all the tests.

Fatigue tests of the prestressed specimens were performed in the same air and tap water environments as used in the standard specimen tests. The results of the fatigue tests are presented in the form of an SN curve in Figure 5.

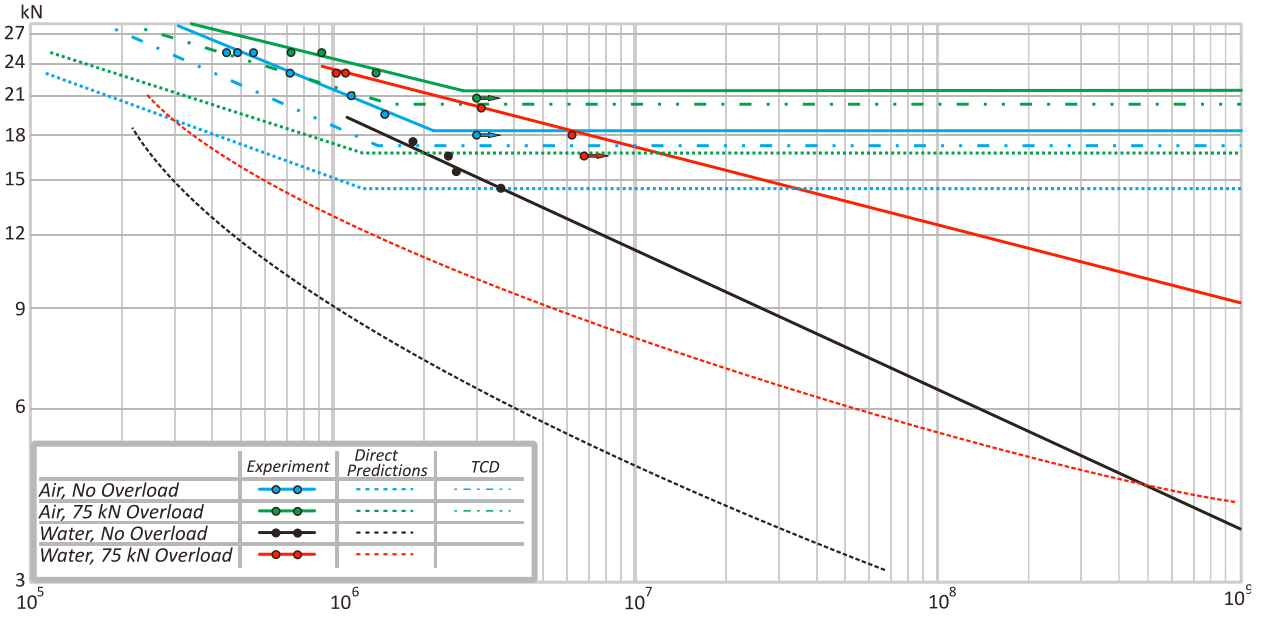

Fig. 5. Experimental and numerical results of the fatigue testing of the double notched samples in terms of applied remote force vs. number of cycles.

Fatigue testing in air

The blue and green lines in Figure 5 represent fatigue test results for double notched specimens in air with and without the overload effect respectively. The prestressed specimens were subjected to a pre-test overload of 75 kN.

Initial inspection of Figure 5 suggests that the autofrettage effect does not result in a major increase in specimen fatigue life. However, for this particular low carbon steel the initial yield stress is less than the fatigue limit for a load cycle with $R = 0$ and compressive residual stress is induced in the notch region during the first load cycle of the fatigue test (i.e. shakedown). Consequently, for this material compressive residual stress is present even without initial overloading.

Fatigue life calculations were performed by conventional stress based assessment procedure and by the critical distance theory method. According the conventional stress based method, calculated stresses at a material point on the surface are directly compared to stresses obtained from uniaxial testing. For the case of the double notched sample the maximum alternating stresses are found at the four corners of the notch intersections. The blue dotted line presents the prediction made by comparing these stresses directly to those from the uniaxial tests on standard specimens. It is seen that these predictions underestimate the fatigue life. This is attributed to the presence of a high

stress gradient in the notched area, so that the stresses rapidly decrease with distance from the stress concentration. It is known that in the situation with high stress concentrations, the fatigue life should be estimated by calculating stresses in a fatigue process volume of material rather than a material point at the component surface.

The blue dash-dot line represents the prediction made by the use of the critical distance method, in which calculated stresses are averaged over some distance from the component surface. There are several options for this method in which the stresses are averaged over either a line, area or volume. In the simplest option, the critical distance is determined with the use of a fracture mechanics approach as follows:

$$L = \frac{1}{\pi}\left(\frac{\Delta K_{th}}{\Delta \sigma_0}\right) \tag{6}$$

where ΔK_{th} is fatigue crack propagation threshold for a given R value and $\Delta\sigma$ is the fatigue limit of a plain sample under a given R value. The prediction of the fatigue limit of a component with stress concentration is then made according to:

$$\Delta\sigma(L/2) = \Delta\sigma_0 \tag{7}$$

It is seen that with the use of the critical distance method the predictions are much closer to the experimental results. In general, stress based assessment methods predict the crack initiation life. The coincidence between the stress based predictions and experimental results for fatigue in air means that the crack initiation life is much longer than the crack propagation life.

Corrosion Fatigue Testing

Unlike the fatigue in air results, the corrosion fatigue testing shows that the overloading the double notched samples gives a major improvement in the fatigue life of the specimens. Given that no fatigue limit occurs in a corrosion environment (or possibly exists at a very low stress level), the fatigue life improvement of the overloaded samples in region of 10^8 –10^9 cycles is even higher. This is due to the difference of the slope of the overloaded and non-overloaded specimen curves. The difference between the air and corrosion fatigue results for the double notched specimens is not as significant as for the standard specimens tested in uniaxial conditions. This may be explained by the fact that in the case of the double notched specimens, if a crack is initiated at notch roots at the same stress level as for the plain specimens, propagation of the crack is significantly retarded by the compressive residual stress field. The numerical predictions made for the corrosion fatigue testing support this assertion. Numerical results obtained by the stress based assessment methodology differ significantly from the experimental results. This is because calculations made by this methodology predict the crack initiation life. The rest of the life is the crack propagation stage, which is dominant in the fatigue life of both overloaded and non-overloaded samples. The next stage of this study will be to perform crack propagation analysis so as to predict corrosion fatigue life as the sum of the crack initiation life and crack propagation life.

4. Conclusions

This study presents experimental results and numerical modelling of the effect of compressive residual stress on the corrosion fatigue life of a low carbon steel. A new approach of evaluating the influence of compressive residual stresses on the fatigue life based on testing of the double notched samples is proposed. The geometry of the double notched sample provides a similar 3D stress-strain distribution to a real pressure part, such that the effects expected from testing a real autofrettaged pressure part is observable in a simpler type of test specimen. This can provide estimation of the influence of compressive residual stresses at an early stage in the design process.

To calculate the compressive residual stress field accurately, the actual material cyclic plasticity response and advanced material modelling techniques are required. Here, a modified plasticity model able to accurately describe the cyclic plasticity response is proposed. The developed model is calibrated to the experimental stress-strain curves obtained for low carbon streel.

The influence of compressive residual stresses on corrosion fatigue life has been assessed through tests on standard and double notch tests specimens in air and tap water environments. Uniaxial fatigue tests on standard specimens with various loading ratios showed significant decrease in fatigue life in the water environment. Parameters from the results of the uniaxial tests were used for the numerical predictions of the fatigue life based on the conventional stress based approach and the critical distance theory.

The results obtained from fatigue tests of double notched samples with the induced compressive residual stress (autofrettage effect) demonstrated an increase in the fatigue life in both the air and corrosion environments. The improvement in the corrosion fatigue life with inducing compressive residual stresses is particularly notable in the very high cycle fatigue region, where the allowable working load is increased by a factor of 2.5 compared to the non-overloaded samples. The numerical predictions of the fatigue lifetime show that the fatigue life of the samples tested in air is mainly based on the crack initiation stage, while for the samples tested in water the crack propagation stage is dominant in the fatigue lifetime.

Acknowledgements

This project has received funding from the European Union's Horizon 2020 research and innovation programme under the Marie Sklodowska-Currie grant agreement No 643159.

References

[1] A. Parker and J. Underwood, Influence of Bauschinger Effect on Residual Stress and Fatigue Lifetimes in Autofrettaged Thick-Walled Cylinders, Fatigue and Fracture Mechanics, 29 (1999) 565-583.
[2] H. Jahed, B. Farshi and M. Hosseini, Fatigue life prediction of autofrettage tubes using actual material behaviour, Int. J. Pressure Vessels and Piping, 83 (2006) 749-755.
[3] R. Adibi-Asl and P. Livieri, Analytical Approach in Autofrettaged Spherical Pressure Vessels Considering the Bauschinger Effect, J. Pressure Vessel Technology, 129 (2007) 411–419.
[4] N. Wahi, A. Ayob and M. K. Elbasheer, Effect of Optimum Autofrettage on Pressure Limits of Thick-Walled Cylinder, Int. J. Environmental Science and Development, 2 (2007) 329–333.
[5] A. Trojnacki and M. Krasiński, Numerical Verification of Analytical Solution for Autofrettaged High-pressure Vessels, J. Theoretical and Applied Mechanics, 52 (2014) 731–744.
[6] E. Herz, O. Hertel and M. Vormwald, Numerical simulation of plasticity induced fatigue crack opening and closure for autofrettaged intersecting holes, Engineering Fracture Mechanics, 78 (2011) 559-572.
[7] R. Thumser, J.W. Bergman and M. Vormwald, Residual stress fields and fatigue analysis of autofrettaged parts, Int. J. Pressure Vessels and Piping, 79 (2002) 113-117.
[8] R. Thumser, J.W. Bergman, E. Herz, O. Hertel and M. Vormwald, Variable amplitude fatigue of autofrettaged diesel injection parts, Mat.-wiss. u. Werkstofftech, 39 (2008) 719-725.
[9] D. Taylor, The Theory of Critical Distances, Elsevier, 2007.
[10] J. Chaboche, K. Dang-Van and G. Cordier, Modelisation of the strain memory effect on the cyclic hardening of 316 stainless steel, S.M.I.R.T. 5 Division L, Berlin, Germany, 1979.
[11] D. Nouailhas et al, On the Description of Cyclic Hardening and Initial Cold Working, Engineering Fracture Mechanics, 21 (1985) 887-895.
[12] N. Ohno, A Constitutive Model of Cyclic Plasticity with a Nonhardening Strain Region, J. Applied Mechanics, 49 (1985) 721-727.